Thermal therapy with a fully electronically steerable HIFU phased array using ultrasound guidance and local harmonic motion monitoring

Pegah Aslani, Leah Drost, Yuexi Huang, Benjamin B. C. Lucht, Erin Wong, Gregory Czarnota, Caitlin Yee, Bo Angela Wan, Vithusha Ganesh, Samuel T. Gunaseelan, Elizabeth David, Edward Chow and Kullervo Hynynen

***Abstract* — The method of localized harmonic motion (LHM) monitoring has been proposed as an ultrasound-based monitoring technique for *in vivo* real-time ultrasound-guidance during thermal surgery. *Objective:* The focus of this paper is to study the performance of LHM monitoring *in vivo* in order to assess the tissue coagulation during ultrasound surgery of bone metastases. This is done through a pre-clinical study on large scale animals (pigs) as well as a first-in-human pilot study, using a hand held ultrasound-guided HIFU phased array. *Methods:* A flat, fully steerable HIFU phased array system (1024 elements, 100 mm diameter, 516 kHz), in combination with a co-aligned 64 element imaging system, is used to perform thermal surgery and monitor tissue coagulation using the LHM technique. The *in vivo* experiments are conducted using thirteen animals, followed by a first-in-human pilot study in which nine patients are enrolled. *Results:* The pre-clinical results show that the LHM monitoring method is able to detect about 80% of the observed coagulated tissue volumes visible in dissection. In the pilot study, six out of nine patients have durable pain reduction with good correlation observed from LHM detections. *Conclusion:* In general, the results suggest that the LHM monitoring performance is promising in detecting thermal tissue coagulation during focused ultrasound surgery in tissues close to the bone. *Significance:* The LHM technique can offer a very accessible and cost-efficient monitoring solution during ultrasound surgery within a clinical setting.**

***Index Terms*— Focused ultrasound, HIFU, local harmonic motion monitoring, phased arrays, stiffness mapping, ultrasound-guided surgery.**

The research in this publication is supported by ORF, OICR, FedDev, and Harmonic Medical.

P. Aslani, B. B. C. Lucht, L. Drost, Y. Huang, E. Wong, C. Yee, B. A. Wan, V. Ganesh, S. T. Gunaseelan are with the Sunnybrook Research Institute, 2075 Bayview Avenue, Toronto, ON M4N 3M5, Canada.

G. Czarnota is with Sunnybrook Research Institute, Sunnybrook Health Sciences Center and, Departments of radiation oncology and medical biophysics at University of Toronto, Toronto, ON, Canada.

E. David is with Sunnybrook Research Institute, Sunnybrook Health Sciences Center and, Department of Medical Imaging at University of Toronto, Toronto, ON, Canada.

E. Chow is with Sunnybrook Research Institute, Sunnybrook Health Sciences Center and, Departments of radiation oncology at University of Toronto, Toronto, ON, Canada.

K. Hynynen is with Sunnybrook Research Institute, Department of Biomedical Physics, and Institute of Biomaterials and Biomedical Engineering at University of Toronto, Toronto, ON, Canada (e-mail: khynynen@ sri.utoronto.ca).

I. Introduction

In recent years, thermal therapy using high-intensity focused ultrasound (HIFU) has shown promise due to its ability to non-invasively treat cancerous cells.

This procedure deposits the focused ultrasound (FUS) energy deep in the tissue while the surrounding tissue remains unharmed. In past years, this technique has been used in numerous treatment cases such as breast [1–4], uterine fibroids [5–9], kidney [10], liver [11], pancreatic [12], prostate [13–16], thyroid cancers [17, 18], and some applications in trans-cranial ablation of the brain [19–20].

Bone is one of the early targets during the metastatic spread of cancer, especially in patients with breast, prostate, lung, and kidney cancer [21 – 23].

About 75% of patients with bone metastatic tumor suffer from severe pain which significantly impacts their quality of life [24, 25]. Hence, there is a challenge to find palliative therapies that can improve the quality of life for these patients. Some of the standard treatments include radiation therapy (RT) along with systematic therapies and analgesics. However, after radiation therapy about 67% of patients will have residual pain. This is the case while some of the patients have already reached their radiation dose limit [26, 27].

This leaves the patients with limited treatment options. There are invasive options such as surgical interventions [28] and percutaneous cryoablation [29]. However, given the fragile state of many of the patients, the longer recovery time, and the higher risk associated with such procedures, not many of the patients qualify for this option. In addition, there are non-invasive options such as use of analgesics. Despite being effective in reducing the pain temporarily, there are adverse long-term side effects associated with this class of drugs that are not desirable to many patients. Therefore, there is a need for alternative palliative therapies for painful bone metastases.

This creates the challenge of finding ways that can improve the quality of life for these patients. Thermal therapy using HIFU has been used in the past to treat bone metastases [2]; in fact, there have been a number of preliminary clinical studies in which HIFU has shown to be safe and effective in palliative care of bone metastases for different groups of patients [21,30-46]. The palliative outcome of HIFU treatment has been associated with multiple mechanisms such as, periosteum loss of nerve supply and nidus vasculature due to ablation, tumor debulking and, reduction of osteoclast-mediated osteolysis

[47, 48].There are significant benefits in using image-guided HIFU; the procedure is completely non-invasive and it can be conducted repeatedly as needed, since there are no concerns in terms of radiation exposure and safety [49, 50].

One of the challenges in using this modality is to be able to assess the progression of tissue coagulation, in order to maintain patient safety.

Currently, magnetic resonance (MR) thermometry is the only FDA approved technique that can offer reliable feedback for assessing tissue coagulation using HIFU systems. However, using MR monitoring can be quite time-consuming and expensive as well as introducing portability constraints that impose limitations on treatment accessibility. There can also be difficulties in placing patients with limited mobility. In addition to its obvious use as a treatment guiding modality, ultrasound imaging can offer a faster, more cost-effective, and portable option for thermal coagulation monitoring.

In 2003, local harmonic motion (LHM) monitoring method was proposed for detecting thermal coagulation of tissue [52]. It is based on radiation force induced tissue motion and can be used to create tissue stiffness maps of the focal volume. In this method [53], an oscillating radiation force is produced by the amplitude variations of the focal intensity of the HIFU transducers resulting in focal tissue oscillation at the modulation frequency. A diagnostic transducer is used simultaneously to assess tissue displacement by repeated ultrasound bursts.

The amplitude of the tissue displacement is correlated with tissue stiffness since the magnitude of the radiation force is kept constant through the treatment. As the tissue coagulates, its stiffness increases and this causes the tissue displacement to drop. Hence coagulation can be detected in real-time by monitoring the tissue displacement during the sonication. Since the LHM method was introduced for the first time, there have been number of successful thermal therapy investigations demonstrating the feasibility of detecting tissue coagulation *in vitro* [54] and *in vivo* [55 – 58].

In this paper, the HIFU transducer used in the LHM monitoring is improved by replacing the single element transducer by a phased array system that allows electronic beam steering. In general, phased arrays have a number of benefits in comparison with single element transducers. For instance electronic steering simplifies treatment planning and targeting (especially for variable depths), can treat multiple areas without adjusting array positioning and, provide control over the focal dimensions [59].This paper is composed of a pre-clinical study as well as a pilot study on a small number of patients.

The objective of the pre-clinical experiments is to study the application of *in vivo* LHM monitoring for tissues that are in vicinity of bone and its potential as a feedback mechanism during thermal therapy in large animals and thus test the methods suitability for human treatments.

For this application, the 1024 element HIFU phased array is used in combination with a co-aligned diagnostic ultrasound transducer for imaging.

Prior to this work, extensive investigation has been done on *in vivo* lesion formation and characterization using MRI and macroscopic examination [53]. In addition, the location of LHM measurements with respect to the lesion are validated by seeing a temperature rise at the focal point using T2-weighted MRI images, while the LHM displacement amplitude dropped. More detailed discussion on lesion characterization is provided in reference [53].

In the current pre-clinical study, one of the objectives is to tune the LHM algorithm for the case of large animal model, which can provide more insight for clinical applications. Hence, a binary outcome is needed to fulfill this objective. In fact, this work is an effort to only rely on a binary feedback from LHM and be able to make a clinical decision as to stop or continue the treatment, without the help of any other modalities.

After assessments on the performance of LHM monitoring during the pre-clinical studies, a pilot study is designed to evaluate the tolerance and safety of performing thermal surgery using HIFU on patients with bone metastases, while storing the LHM signals for post-treatment analysis. The results from the pre-clinical study are used for lesion assessment in the first-in-human pilot study. In order to assess the effectiveness of the treatments and accuracy of the LHM monitoring technique, pain reduction and quality of life is assessed for each patient. It is shown that the HIFU treatment using this device is safe for the patients, while no serious side effects were observed.

II. MATERIALS AND METHODS

A. *Transducer array*

In order to induce thermal ablation and local harmonic motion in the tissue and conduct LHM monitoring during treatment, an in-house manufactured 1024 element phased array system is used [60, 61]. The transducer head has an outer diameter of 100 mm and a central hole of 24 mm diameter to accommodate an ultrasound imaging probe. The focus is in shape of an ellipsoid and, at a focal depth of 3 cm from the transducer, the beam width (at 50% of the maximum pressure amplitude) is 2 mm and the beam depth of field is 11 mm [62].

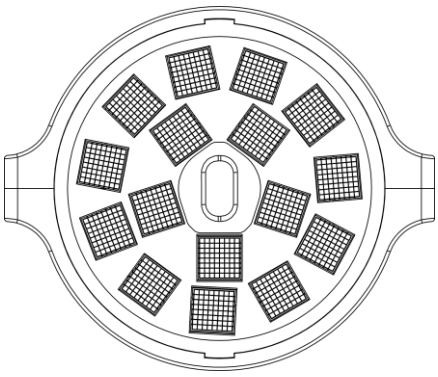

Fig. 1. The 1024 element array used for HIFU ablation with the imaging probe mounted in the center.

Figure 1 shows the transducer array head with the imaging probe mounted in the center, such that it is co-aligned with the HIFU phased array. The imaging probe is a commercial 64 element phased array with a 5 MHz center frequency and a width of 24 mm (PA7-4/12, Ultrasonix Inc., Canada). It operates in M-mode during the LHM monitoring.

The *in vivo* experiments are conducted using the in-house built driving system. Figure 2 shows the schematic of different components of the system in the experimental set-up for HIFU ablation and the LHM monitoring.

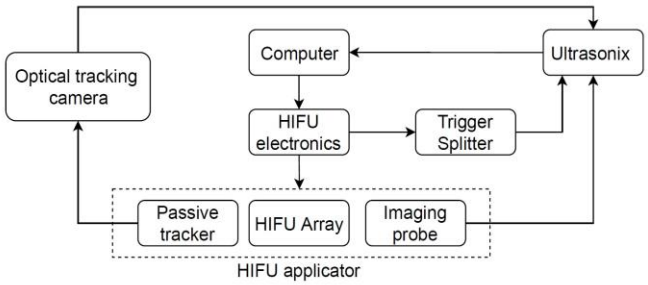

Fig. 2. Block diagram of the experimental set-up.

The system is composed of a main computer which is responsible for the HIFU array as well as the imaging probe. A function generator (WGM-201, Syscomp Electronic Design, Canada) operates as a trigger splitter to convert a single pre-burst trigger into A-line trigger signals for the Ultrasonix imaging system. The Ultrasonix (SonixTouch, Ultrasonix, Canada) is a clinical imaging platform that provides a control interface for the imaging probe. Custom software is run on the Ultrasonix to communicate with the 3D optical tracker (Northern Digital Inc., Canada) in order to keep track of any motion of the transducer head, and to pass the imaging data back to the main computer.

B. Treatment workflow

The transducer array is excited at its central frequency of 516 kHz. During LHM monitoring, the HIFU signal is amplitude modulated at 50 Hz using a 50% duty cycle square wave. This modulation frequency is chosen to obtain higher displacement amplitudes [53] in the tissue in order to make displacement detection easier, at the cost of a longer time to complete a full motion cycle. Due to the square wave modulation, the displacements in every cycle are composed of a push segment and a relaxation segment. During each LHM push/relaxation cycle the imaging probe is excited through the trigger splitter at 1 kHz pulse repetition frequency, resulting in 20 A-lines for each cycle.

The treatment procedure includes 3 different stages: a pre-treatment-baseline, treatment and a post-treatment-baseline. In a pre-treatment-baseline, the stiffness of the untreated tissue is assessed through displacement amplitudes. During the treatment stage, LHM monitoring for stiffness assessment is conducted on a 3s interval, with the intervening period occupied with continuous wave HIFU application at the treatment power. Thus the treatment duration is divided into multiple fractions of time, with LHM fractions and treatment (or CW) fractions alternating until the treatment is completed. By alternating these fractions, the tissue stiffness, and consequently lesion formation, can be monitored throughout the treatment.

In the last stage, once the treatment is finished, the stiffness amplitude of the treated tissue is obtained by acquiring a post-treatment measurement in the same manner as the pre-treatment baseline.

In this system, every LHM monitoring fraction consists of five 20 ms push-relax cycles, corresponding to 100 A-lines. This is equivalent to 100 ms of monitoring time. Including overhead for mode switching from one fraction to the other, the LHM fractions lasts approximately 150 ms. It uses an acoustic power of 116 W for the push cycles. This is the maximum acoustic power provided by the device; it is chosen to ensure that the maximum radiation force is applied during monitoring.

C. Displacement assessment

After the treatment session is completed, the data are analyzed offline. The received radio-frequency (RF) signals are first filtered through a digital high-pass filter and a series of notch filters in order to remove the HIFU interference at its excitation frequency as well as all its harmonic components. Using a residual sum of squares [63] as a cross-correlation technique between each pair of sequential A-lines in the fraction, the time delay between consecutive A-lines is calculated. The center of the cross correlation window is chosen close to the focus, but in such a way that it does not include the bone echo.

Having calculated the delay between each two consecutive A-lines, and knowing the speed of sound in the tissue, one can calculate the displacement distance corresponding to each time point. Hence, it is possible to reconstruct the push and relaxation cycles based on this method.

Figure 3 shows an example of displacements from one sonication.

Additionally, displacement amplitudes in every cycle can be found by looking at the displacement resulting from the push or by looking at both push and relaxation segments of the cycle.

One of the possible artifacts that can present itself in the push and relaxations in the displacement through time is the background motion such as breathing, or slow movements of the subject. Thus, in order to determine the displacement amplitudes, the background motion should be taken into account.

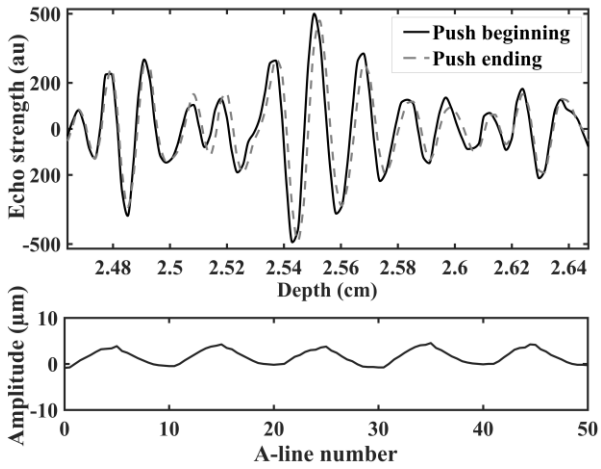

Fig. 3. Top: Windowed echo signal at the focus in the beginning and end of push. Bottom: Displacements through one fraction including five sonications.

Once the amplitudes are calculated in every fraction while eliminating artifacts, one can see the variations of displacement amplitude and hence tissue stiffness throughout the treatment. A simple protocol for a lesion assessment is to declare a lesion whenever the displacement amplitude drops below a certain threshold. Having obtained a pre-treatment-baseline, the standard deviation of the displacement amplitudes is calculated. A lesion is assessed whenever the displacement amplitude during the treatment falls below the averaged maximum displacement by a multiple of the standard deviation of the pre-treatment-baseline. Receiver operating characteristic (ROC) analysis is done in order to evaluate the diagnosis ability of the LHM monitoring as well as finding the optimal threshold value for lesion assessment. In order to test the accuracy of the LHM monitoring, a pre-specified value of 0.5 is reserved for the area under the curve (AUC_0). In this case, the null hypothesis is that the AUC is less or equal to AUC_0, (i.e. the LHM monitoring is not a useful discriminator). The null hypothesis is tested based on the methods introduced by Hanley and McNeil [64].

True positive rate (TPR), i.e. sensitivity, and false positive rate (FPR), i.e. specificity, are calculated for the coagulation detection, determined from the dissection as the gold standard. Using the ROC curve, the optimal threshold value is determined with the Youden index [65] method, which maximizes the difference between TPR and FPR.

D. In vivo pre-clinical experiments

In order to evaluate the performance of the LHM monitoring as well as the new transducer system *in vivo*, a porcine model is chosen to accommodate a large number of treatment locations and to test a clinically relevant range of tissue thicknesses. The experiments are done under Institutional Animal Care committee approval.

In all, tests are done on 13 subjects, ranging from 30-50 kg. The pigs are anaesthetized with a ketamine/atropine mixture and the region to be sonicated is shaved, chemically depilated, and thoroughly washed with water and soap. The pigs are intubated and anesthesia is maintained with 2-4% isoflurane for the duration of treatment. Next, the integrated transducer system is coupled acoustically to the target area using a bag of degassed and deionized water and a degassed solution of deionized water and ultrasound gel. Using the imaging probe in the center of the transducer array, the target area is imaged to find the bone. Once the target area is identified, the transducer array is held in place using a locking mechanical arm. For some treatments, the ventilator is stopped to force a breath hold for the treatment duration. This is done to try to identify the effect of breathing motion on the displacements. Once the experiment is finished the animals are euthanized and dissected to visually verify the effects of the treatment.

Figure 4 on the left shows the B-mode image of the bone before the treatment. The image on the right shows the B-mode image of the bone after the treatment where the lesion is observed.

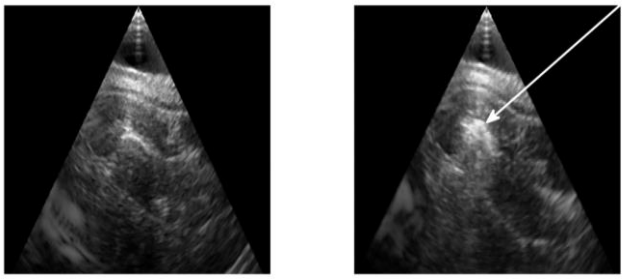

Fig. 4. Left: B-mode image of the bone before the sonication. Right: B-mode image of the bone after the sonication, where the lesion is indicated by the arrow.

E. Population for the pilot study

The focus of the clinical-trial is to conduct a pilot study to investigate the safety and efficacy of using USgHIFU as a palliative therapy for patients with bone metastases. Preceding the clinical trials, institutional research ethics board approval is obtained (REB # 005-2014). Starting March 2017 to August 2018, 9 patients with bone metastases are enrolled in the clinical trial at Sunnybrook Health Sciences Center, Toronto, Canada. Informed consent is granted by each of the enrolled patients. The state of malignancy for each patient is previously confirmed through either histology or cytology.

The criteria upon which the patients are selected required the patients to be able to record daily pain levels as well as medication dosage. Radiographic evidence of bone metastases correlated to the painful site is needed for treatment, given that treatment site is accessible to HIFU treatment based on the imaging data. In addition, the patients' baseline pain score has to be at least 2 or higher on a scale of 0 to 10.

F. Treatment procedure

Preceding the treatment, the baseline pain score is recorded for every patient. In addition, the tumor area to be treated is measured and recorded, as well as the use of analgesics. In order to confirm the accessibility as well as safety of the treatment, the tumor location is confirmed either through MRI

or ultrasound on the same day as the thermal surgery. Prior to the treatment, patients received light intravenous (IV) sedation as well as local anesthesia at the treatment site (Marcaine 2%). As a safety protocol, vital signs, such as blood pressure, heart rate, and oxygen saturation are recorded during the treatment. Meanwhile, patients are positioned optimally in such a way that the treatment site is easy to reach and a clear pathway for HIFU, which is confirmed by ultrasound imaging throughout the procedure, is provided. Once, the tumor location is verified, and sufficient acoustic coupling to the skin is provided – using a degassed water pad and degassed coupling gel solution – the transducer head is positioned over the treatment area and the mechanical arm is locked to avoid any movement. Subsequently, the HIFU focus – as well as the focus for LHM monitoring – is located slightly above the bone. The acoustic power is adjusted to the maximum tolerable power by the patient. Next, multiple points at the adjusted power are sonicated and monitored. The schematic of this configuration is shown in Figure 5.

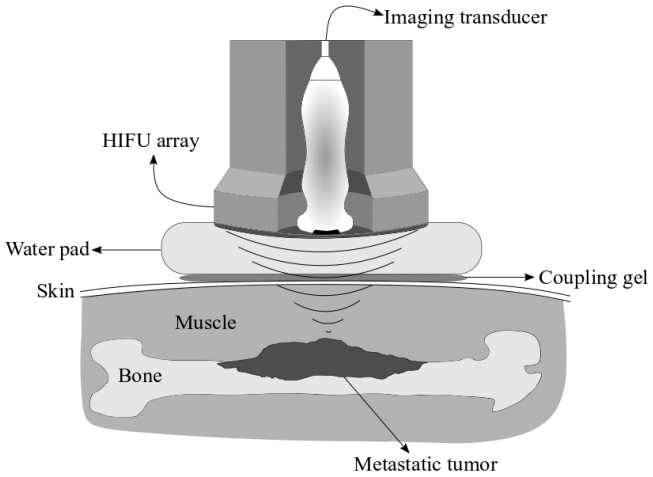

Fig. 5. The configuration of the combined HIFU and imaging arrays with respect to the bone during the treatment.

III. RESULTS

A. *Pre-clinical experiments*

Target locations on the surface of ribs, leg bones and spine are chosen. A total of 179 sonications are carried out on the subjects. The acoustic power during the sonications is chosen between 11 and 78 W for durations between 25 and 80 s in order to explore the range of thermal exposures that could induce thermal coagulation on the bone surfaces. Out of 179 total number of sonication points, in 135 locations thermal coagulation is observed in post-mortem histology, i.e. there is about 75% prevalence rate for coagulation at the exposures used.

In order to be able to quantify the performance of LHM monitoring the results are classified into four cases of true positive (TP), false positive (FP), false negative (FN) and, true negative (TN).

Thermal coagulation detection using LHM monitoring is assessed for different threshold values set by varying the multiplicative factor of the pre-treatment-baseline amplitude standard deviation. The results are used to obtain the ROC curve which is shown in Fig. 6.

TABLE I
SONICATION PARAMETERS FOR THE EXPERIMENTS USING OPTIMAL THRESHOLD VALUE.

	HIFU power (W)	Focal depth (cm)	Treatment duration	Treatment points	# of thermal coagulations	Coagulations accurately detected
Pig 1	11 – 66	2.23 – 2.96	45 – 65	19	12	11
Pig 2	44 – 66	2.31 – 4.51	45	9	9	9
Pig 3	49 – 73	2.01 – 4.19	45	14	13	9
Pig 4	49 – 73	2.58 – 3.31	25 – 45	12	12	9
Pig 5	73	2.49 – 3.51	30 – 45	11	8	6
Pig 6	49 – 73	2.25 – 4.18	45	20	19	9
Pig 7	36 – 73	2.13 – 4.99	45	10	4	4
Pig 8	17 – 73	2.41 – 4.54	45 – 95	16	9	8
Pig 9	19 – 73	2.79 – 4.80	16 – 21	17	9	9
Pig 10	19 – 73	2.72 – 5.53	21	19	15	14
Pig 11	19 – 73	2.40 – 4.08	21	20	14	10
Pig 12	36 – 73	2.39 – 5.39	21	6	5	5
Pig 13	73	3.59 – 6.41	21	6	6	5

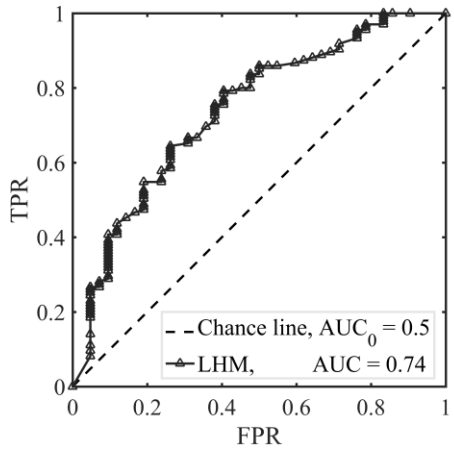

Fig. 6. ROC curve for LHM monitoring.

Having done the ROC analysis for the LHM monitoring based on the gold standard, the AUC is calculated to be 0.74 with the 95% confidence interval: 0.66-0.82and *p*-value less than 0.00001. In addition, the coefficient of variation of the AUC is less than 3.9%. The results suggest that the null hypothesis can be rejected, i.e. the LHM monitoring technique is significantly different than the chance line and therefore a good discriminator of lesion formation.

The optimal threshold value is obtained as 3.85 times the standard deviation of the pre-treatment-baseline. Choosing this threshold value for LHM monitoring, the system is able to detect about 80% of the observed thermal coagulation according to the gold standard. In addition the FP, TN and FN rates are obtained as 45%, 55% and 20%, respectively.

Using the optimal threshold value, the results of animal study as well as the sonication parameters for each case are summarized in Table I. Here, the focal depths are measured with respect to the HIFU array.

Moreover, it is interesting to study the number of true detections as well as the number of false detections for different depth and power ranges. This result is shown in Figure 7. Here, true detection includes both the number of TPs and TNs and, similarly, false detection includes both FPs and FNs. Adding the number of true detections and false detections corresponds to the total percentage of sonications at that depth and power range.

TABLE II
TUMOR SIZE AND LOCATION FOR EVERY PATIENT

	Tumor Size (cm)	Tumor Site
Patient 1	5.6 × 5.0	Rib
Patient 2	4.5 × 1.9	Ulna
Patient 3	2.0 × 1.1	Rib
Patient 4	2.8 × 1.6	Scapula
Patient 5	4.8 × 1.4	Rib
Patient 6	2.0 × 1.0	Rib
Patient 7	5.2 × 3.5	Iliac crest
Patient 8	2.4 × 1.8	Scapula
Patient 9	1.4 × 1.3	Humerus

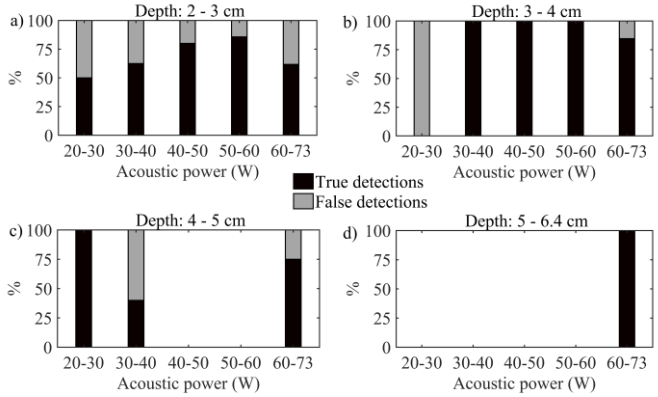

Fig. 7. Percentage of true and false detections for different depths and power ranges.

The results in Figure 7 suggest that there is no explicit trend for the percentage of true and false detections for different depths. It is interesting to note that in Figure 7a, the percentage of false detections typically decreases with the increase in the acoustic power. However, at higher values of power, i.e. 60 – 73 W, the percentage of false detections has slightly increased. One should consider that strong vaporization effects and gas activity are more probable at higher acoustic power which can affect the detection accuracy.

B. Clinical trials

In general, the treatment locations include extremities, scapula, rib and iliac bones. The treatment locations, as well as the tumor size are described in more detail in Table II for every patient. During the procedure, two stop buttons are available and the treatment relies on the feedback provided by the patient. The treatment would stop either because patient felt significant pain at the treatment location and pushes the

TABLE III
SONICATION PARAMETERS AND PATIENTS' OUTCOME

	HIFU Power (W)	Focal Depth (cm)	Treatment duration (s)	# Sonications	# Lesions detected by LHM	Pain reduction
Patient 1	30.9 – 42.1	2.65 – 2.94	20 – 30	2	0	Not durable
Patient 2	30.6 – 37.4	3.37 – 3.69	20	4	2	Not durable
Patient 3	30.6 – 44.8	2.50 – 2.99	20	8	1	Durable
Patient 4	30.6	2.40 – 2.90	20	2	0	Durable
Patient 5	30.6 – 41.0	3.04 – 3.41	20	9	4	Durable
Patient 6	35.1 – 45.9	2.30 – 2.93	20 – 30	10	4	Durable
Patient 7	44.5 – 52.2	3.53 – 4.74	20 – 35	7	1	Not durable
Patient 8	19.8 – 25.0	2.69 – 3.10	20 – 30	7	2	Durable
Patient 9	6.70 – 8.30	3.79 – 4.11	15 – 25	8	2	Durable

stop button, or something moves and the treatment is stopped by the operator. If none of the stop buttons are used during the treatment, the treatment would continue until the pre-set time is completed. The LHM monitoring data are processed off-line.

The number of lesions predicted by LHM along with sonication parameters is listed for each patient in Table III. At the end, the patients' pain score is recorded for 10 days post treatment. Moreover, the treatment durability is assessed by patient follow up and if the patients need to receive RT after the HIFU treatment, which is also recorded in Table III. The treatment duration is composed of sonication time as well as the time spent for LHM monitoring.

The top graph in Figure 9 shows a case where amplitude has dropped below the threshold and a lesion is detected and, the graph in the bottom shows a case where no lesion is detected where the displacement amplitude does not drop sufficiently.

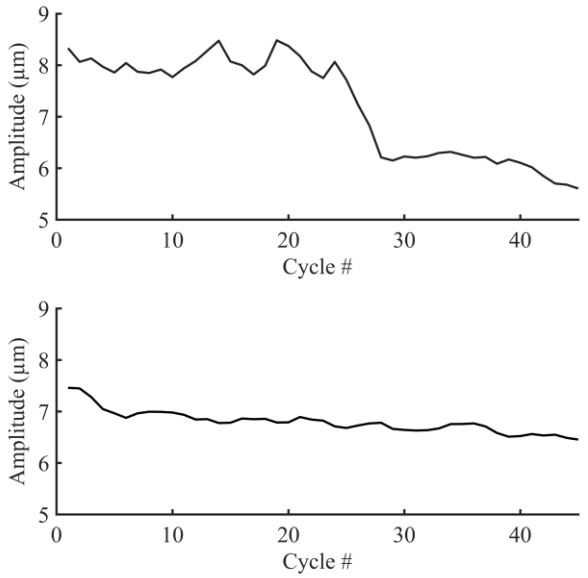

Fig. 9. The displacement amplitudes Top) lesion is detected Bottom) no lesion is detected.

Overall, 6 out of 9 patients have durable pain reduction after the HIFU treatment. All patients who do not have durable pain reduction receive RT sometime after the HIFU treatment.

IV. Discussion

In this paper, a flat electronically steerable HIFU phased array with frequency of 516 kHz along with a co-aligned imaging phased array is used to investigate the diagnostic ability of LHM monitoring for lesion formation through a pre-clinical study. The flat HIFU array is successful in heating and ablating the tissue. Using this array the focus can be easily adjusted to different depths and lateral locations visible with the imaging probe. In addition, the LHM system is also successful in inducing the harmonic displacements in the tissue and monitoring them in vivo.

In the pre-clinical stage, the results from the ROC analysis support further investigation of using LHM as a real-time monitoring technique in detecting lesion formation for HIFU applications, especially in enhancing the TRP while trying to decrease the FPR mainly caused by physical decorrelations and strong vaporization effects during the treatment procedure. In addition, decorrelations between pre-treatment-baseline and the treatment can also be another possible cause of false detections. The variations of the standard deviation of the pre-treatment baselines (σ) are summarized in Table IV by taking the mean (η) and standard deviation (ϵ) of σ for each category of TP, FN, FP, TN.

The results in Table IV suggest similar variation parameters for categories of TP and FP. In addition, the variation parameters are significantly higher for FN and TN categories. The higher mean value for FN category makes the algorithm insensitive to the actual drop caused by the lesion. On the other hand, the lower mean value for FP category (which is similar to the TP category), makes the algorithm sensitive to random noise. Moreover, it is important to note that in these experiments, the treatments extended past the time point where LHM detected the lesion; future work will integrate the LHM feedback into the treatment control and test whether turning off the HIFU at lesion detection is effective [40].

TABLE IV
VARIATIONS OF σ FOR EACH CATEGORY

Result	η (μm)	ϵ (μm)
TP	0.87	1.35
FP	0.87	1.08
FN	1.75	2.72
TN	3.51	7.06

The results from the first-in-human pilot study are promising. In general, good correlation is observed between the LHM detections and the patients' outcome in terms of pain reduction. It is interesting to note that the patients who do not have durable pain reduction have much larger tumor sizes relative to the patients who have durable results. For example, patient 6, for whom LHM detected 4 lesions, has complete pain relief. Assuming an estimate of the average lesion area to be 0.5 cm^2 (based on pre-clinical results), the total lesion area created is similar in size to the tumor area for patient 6.

In addition, patients who do not have durable pain reduction have much higher baseline pain scores and as a result, it is hard for them to stay motionless during the treatment. This can enhance physical decorrelation both in terms of detection as well as energy deposition.

Overall, the prototype device can be improved by increasing the sonication frequency resulting in larger tissue displacements. Similarly the ultrasound imaging is not ideal and higher quality imaging system can potentially improve the image quality and the motion detection.

V. Conclusion

This study demonstrates that a combination of electronically steered phased array with clinical diagnostic ultrasound system can be used to coagulate tissues at bone surface in large animal model as well as in clinical settings. The imaging

system is programmed to acquire M-mode scans through the HIFU focus and it is demonstrated that tissue motion induced by the radiation force from the pulsed ultrasound field can be detected. The detected tissue motion provides a reasonable indicator for tissue coagulation both in pre-clinical investigation as well as the first-in-human pilot study.

ACKNOWLEDGMENT

The research in this publication is supported by ORF, OICR, FedDev, and Harmonic Medical.

We would also like to show our gratitude to Mohammad Kazem, Ping Wu, and Rohan Ramdoyal for their help in building the LHM system; Shawna Rideout-Gros and Alex Garces for helping with the animal experiments; and Dr. John Hudson, Dr. Nicholas Ellens, and Brigitte Babin for assisting with data collection.

REFERENCES

[1] K. Hynynen, *et al.*, "MR imaging-guided focused ultrasound surgery of fibroadenomas in the breast: a feasibility study," *Radiology*, vol. 219, no. 1, pp. 176 – 185, Apr. 2001.

[2] F. Wu, *et al.*, "Tumor vessel destruction resulting from high-intensity focused ultrasound in patients with solid malignancies," *Ultrasound in Med. & Biol.* Vol. 28, no. 4, pp. 535 – 542, Dec. 2002.

[3] F. Wu, *et al.*, "A randomized clinical trial of high-intensity focused ultrasound ablation for the treatment of patients with localized breast cancer," *Br. J. Cancer*, vol. 89, no. 12, pp. 2227 – 2233, Sep. 2003.

[4] D. B. Zippel, and M. Z. Papa, "The use of MR imaging-guided focused ultrasound in breast cancer patients; a preliminary phase one study and review," *Br. Cancer*, vol. 12, no. 1, pp. 32 – 8, Jan. 2005.

[5] E. A. Stewart, "Uterine fibroids," *Lancet*, vol. 357, no. 9252, pp. 293 – 298, Jan. 2001.

[6] C. M. C. Tempany, *et al.*, "MR imaging-guided focused ultrasound surgery of uterine leiomyomas: a feasibility study," *Radiology*, vol. 226, no. 3, pp. 897 – 905, Mar. 2003.

[7] F. M. Fennessy, and C. M. Tempany, "A review of magnetic resonance imaging-guided focused ultrasound surgery of uterine fibroids," *Magn. Reson. Imag.*, vol. 17, no. 3, pp. 173 – 179, Jun. 2006.

[8] M. O. Kohler, *et al.*, "Volumetric HIFU ablation under 3D guidance of rapid MRI thermometry," *Med. Phys.*, vol. 36, no. 8, pp. 3521 – 3535, Aug. 2009.

[9] L. Zhang, *et al.*, "Feasibility of magnetic resonance imaging-guided high intensity focused ultrasound therapy for ablating uterine fibroids in patients with bowel lies anterior to uterus," *Eur. J. Radiol.*, vol. 73, no. 2, pp. 396 – 403, Feb. 2010.

[10] K. U. Kohrmann, *et al.*, "High Intensity Focused Ultrasound as Noninvasive Therapy for Multilocal Renal Cell Carcinoma: Case Study and Review of The Literature," *J. Urol.*, vol. 167, no. 6, pp. 2397 – 2403, Jun. 2002.

[11] F. Wu, *et al.*, "Extracorporeal high intensity focused ultrasound ablation in the treatment of patients with large hepatocellular carcinoma," *Ann. Surg. Oncol.*, vol. 11, no.12, pp. 1061 – 1069, Dec. 2004.

[12] F. Wu, *et al.*, "Feasibility of US-guided high-intensity focused ultrasound treatment in patients with advanced pancreatic cancer: Initial experience," *Radiology*, vol. 236, no. 3, pp. 1034 – 1040, Sep. 2005.

[13] X. Rebillard, *et al.*, "Transrectal high-intensity focused ultrasound in the treatment of localized prostate cancer," *J. Endourol.*, vol. 19, no. 6, pp. 693 – 701, Jul. 2005.

[14] A. Blana, *et al.*, " First analysis of the long-temr results with transrectal HIFU in patients with localized prostate cancer," *Eur. Urol.*, vol. 53, no. 6, pp. 1194 – 1203, Jun. 2008.

[15] M. Warmuth, *et al.*, "Systematic review of the efficacy and safety of high-intensity focused ultrasound for the primary and salvage treatment of prostate cancer," *Eur. Urol.*, vol. 58, no. 6, pp. 803 – 815, Dec. 2010.

[16] R. Chopra, *et al.*, "MR imaging-controlled transurethral ultrasound therapy for conformal treatment of prostate tissue: initial feasibility in humans," *Radiology*, vol. 265, no. 1, pp. 303 – 313, Oct. 2012.

[17] R. D. Kovatcheva, *et al.*, "High-intensity focused ultrasound to treat primary hyperparathyroidism: a feasibility study in four patients," *Am. J. Roentgenol.*, vol. 195, no. 4, pp. 830 – 835, Oct. 2010.

[18] O. Esnault, *et al.*, "High-intensity focused ultrasound ablation of thyroid nodules: first human feasibility study," *Thyroid*, vol. 21, no. 9, pp. 965 – 973, Aug. 2011.

[19] W. J. Elias, *et al.*, "A pilot study of focused ultrasound thalamotomy for essential tremor," *New Engl. J. Med.*, vol. 369, pp. 640 – 648, Aug. 2013.

[20] N. Lipsman, *et al.*, "MR-guided focused ultrasound thalamotomy for essential tremor: a proof of concept study," *Lancet Neurol.*, vol. 12, no. 5, pp. 462 – 468, May 2013.

[21] R. Catane, *et al.*, "MR-guided focused ultrasound surgery (MRgFUS) for the palliation of pain in patients with bone metastases – preliminary clinical experience," *Ann. Oncol.*, vol. 18, no. 1, pp. 163-167, Jan. 2007.

[22] Sh. Li, *et al.*, "Estimated number of prevalent cases of metastatic bone disease in the US adult population," *Clin. Epidemiol.*, vol. 4, pp. 87 – 93, Apr. 2012.

[23] U. Falkmer, *et al.*, "A systematic overview of radiation therapy effects in skeletal metastases," *Acta Oncol.*, vol. 42, no. 5 – 6, pp. 620 – 633, Jan. 2003.

[24] E. Chow, *et al.*, "Quality of life and symptom end points in palliative bone metastases trials," *Clin. Oncol.*, vol. 18, no. 1, pp. 67 – 69, Feb. 2006.

[25] R. McDonald, *et al.*, "Incidence of pain flare in radiation treatment of bone metastases: A literature review," *J. Bone Oncol.* , vol. 3, no. 4, pp.84 – 89, Oct. 2014.

[26] E. Chow, *et al*., "Palliative radiotherapy trials for bone metastases: a systematic review," *J. Clin. Oncol.* , vol. 25, no. 11, pp. 1423 – 1436 , Jan. 2007.

[27] W.F. Hartsell, *et al*., "Randomized trial of short- versus long-course radiotherapy for palliation of painful bone metastases," *J. Natl. Cancer Inst.*, vol. 97, no.11, pp. 798 – 804 , Jun 2005.

[28] M. Ratasvuori, *et al*., "Insight opinion to surgically treated metastatic bone disease: Scandinavian Sarcoma Group Skeletal Metastasis Registry report of 1195 operated skeletal metastasis," *Surg. Oncol.* , vol. 22, no. 2, pp. 132 – 138, 2013.

[29] M. R. Callstrom, , *et al*., "Percutaneous image-guided cryoablation of painful metastases involving bone: multicenter trial," *Cancer*, vol. 119, no. , pp. 1033 – 1041, Oct. 2012.

[30] D. Gianfelice, *et al.*, "Palliative treatment of painful bone metastases with MR imaging-guided focused ultrasound," *Radiology*, vol. 249, no. 1, pp. 355 – 363, Oct. 2008.

[31] B. Liberman, *et al.*, "Pain palliation in patients with bone metastases using MR-guided focused ultrasound surgery: a multicenter study," *Ann. Surg. Oncol.*, vol. 16, no. 1, pp. 140 – 146, Jan. 2009.

[32] G. Orgera, *et al.*, "US-guided high-intensity focused ultrasound of bone and soft tissues metastases: early clinical experience in palliation of chronic pain," *Cardiovasc. Intervent. Radiol.*, vol. 33, no. 2, pp. 274 – 275, 2010.

[33] C. Li, *et al*., "Noninvasive treatmenr of malignant bone tumors using high-intensity focused ultrasound," *Cancer*, vol. 116, no. 16, pp. 3934 – 42, 2010.

[34] G. Orgera, *et al.*, "High-intensity focused ultrasound (HIFU) in patients with solid malignancies: evaluation of feasibility, local tumour response and clinical results," *Radiol. Med.*, vol. 116, no. 5, pp.734 – 748, Aug. 2011.

[35] V. G. Turkevich, *et al.*, "Treatment of painful bone metastases with magnetic resonance guided focused ultrasound," *Eur. J. Cancer*, vol. 47, no. 1, pp. S227 – S228, Sep. 2011.

[36] M. Kawasaki, *et al.*, "Efficacy of magnetic resonance-guided focused ultrasound surgery for bone metastases pain palliation," in: Y.

Matsumoto, L. A. Crum, G. R. TerHaar, eds. *10th Int. Symp. Therapeut. Ultrasound*, pp. 488-492, 2011.

[37] T. Carteret, *et al.*, "MR-guided high intensity focused ultrasound for palliation of bone metastases," *Cardiovasc. Intervent. Radiol.*, vol. 34, no. 3, p. 539, 2011.

[38] E. Weeks, *et al.*, "MRI-guided focused ultrasound (MRgFUS) to treat facet joint osteoarthritis low back pain – case series of an innovative new technique," *Eur. Radiol.*, vol. 22, no. 12, pp. 2822 – 2835, Dec. 2012.

[39] R. Catane, *et al.*, "Pain palliation of bone metastases using magnetic resonance guided focused ultrasound – multi-center multi-trial results," Poster presented at: ESMO Congress, Vienna, Austria, October 1, 2012.

[40] A. Napoli, *et al.*, "Osteoid osteoma: MR-guided focused ultrasound for entirely noninvasive treatment," *Radiology*, vol. 267, no. 2, pp. 1 – 8, May 2013.

[41] A. Napoli, *et al.*, "Primary pain palliation and local tumor control in bon metastases treated with magnetic resonance-guided focused ultrasound," *Invest. Radiol.* vol. 48, no. 6, pp.351 – 358, Jun. 2013.

[42] D. Geiger, *et al.*, "MR-guided focused ultrasound (MRgFUS) ablation for non-spinal osteoid osteoma treatment: a prospective multicenter evaluation," *J. Therap. Ultrasound*, vol. 2, no. 1, p. A24, Oct. 2013.

[43] M. Huisman, *et al.*, "Feasibility of volumetric MRI-guided high intensity focused ultrasound (MR-HIFU) for painful bone metastases," *J. Therap. Ultrasound*, vol. 12, no. 16, pp. 1 – 10, Oct. 2014.

[44] M. D. Hurwitz, *et al.*, "Magnetic resonance – guided focused ultrasound for patients with painful bone metastases: phase III trial results," *J. Natl. Cancer Inst.*, vol. 106, no. 5, pp. 1 – 9, Mar. 2014.

[45] B. Joo, *et al.*, "Pain palliation in patients with bone metastases using magnetic resonance-guided focused ultrasound with conformal bone system: a preliminary report," *Yonsei Med. J.*, vol. 56, no. 2, pp. 503 – 509, Mar. 2015.

[46] M. Chan, *et al.*, "Magnetic resonance-guided high-intensity focused ultrasound for palliation of painful skeletal metastases: A pilot study," *Technology in Cancer Research & Treatment*, vol. 16, no. 5, pp. 570 – 576, Oct. 2017.

[47] S. Dababou, *et al.*, "High-intensity focused ultrasound for pain management in patients with cancer," *Radiographics*, vol. 38, no. 2, pp. 603 – 623, Mar. 2018.

[48] M. J. Temple, *et al.*, "Establishing a clinical service for the treatment of osteoid osteoma using magnetic resonance-guided focused ultrasound: overview and guidelines," *J. Therapeut. Ultrasound*, pp. 4 – 16, May 2016.

[49] M. S. Rovella, *et al.*, "Magnetic resonance guided high-intensity focused ultrasound ablation of osteoid osteoma: a case series report," *Ultrasound Med. Biol.*, vol. 42, no. 4, pp. 919 – 923, Apr. 2016.

[50] C. Masciocchi, *et al.*, "Radiofrequency ablation versusmagnetic resonance guided focused ultrasound surgery for minimally invasive treatment of osteoid osteoma: a propensity score matching study," *Eur. Radiol.*, vol. 26, no. 8, pp. 2472 – 2481, Aug. 2016.

[51] M. S. Rovella, *et al.*, "Magnetic resonance guided high-intensity focused ultrasound ablation of osteoid osteoma: a case series report," *Ultrasound Med. Biol.*, vol. 42, no. 4, pp. 919 – 923, Apr. 2016.

[52] E. E. Konofagou, and K. Hynynen, " Localized harmonics motion imaging: theory, simulations and experiments," *Ultrasound in Med. & Biol.*, vol. 29, no. 10, pp. 1405 – 1413, Oct. 2003.

[53] L. Curiel, *et al.*, "In vivo monitoring of focused ultrasound surgery using local harmonic motion," *Ultrasound in Med. & Biol.*, vol. 35, no. 1, pp. 65 – 78, Jan. 2009.

[54] C. Maleke, and E. E. Konofagou, "Harmonic motion imaging for focused ultrasound (HMIFU): a fully integrated technique for sonication and monitoring ablation in tissue," *Phys. Med. Biol.*,vol. 53, no. 6, pp. 1773 – 1793, Mar. 2008.

[55] J. Heikkila, *et al.*, "A simulation model for local harmonic motion monitoring of focused ultrasound surgery," 8th international symposium on therapeutic ultrasound, September 10 – 13, 2008; in *AIP Conf. Proc.*, New York, NY, USA, 2009, vol. 1113, pp. 190 – 194.

[56] L. Curiel, *et al.*, "Focused ultrasound treatment of VX2 tumors controlled by local harmonic motion," *Phys. Med. Biol.*, vol. 54, no. 11, pp. 3405 – 3419, Jan. 2009.

[57] C. Maleke, and E. E. Konofagou, "Feasibility of real-time monitoring of focused ultrasound surgery (FUS) using harmonic motion imaging (HMI)," *IEEE Trans. Biomed. Eng.*, vol. 57, no. 1, pp. 7 – 11, Jan. 2010.

[58] L. Curiel, and K. Hynynen, "Localized harmonic motion imaging for focused ultrasound surgery targeting," *Ultrasound in Med. & Biol.*, vol. 37, no. 8, pp. 1230 – 1239, Aug. 2011.

[59] K. Hynynen, and R. M. Jones, "Image-guided ultrasound phase arrays are a disruptive technology for non-invasive therapy," *Phys. Med. Biol.*, vol. 61, no. 17, pp. R206 – R248, Sep. 2016.

[60] N. P. K. Ellens, *et al.*,"A novel, flat, electronically-steered phased array transducer for tissue ablation: preliminary results," *Phys. Med. Biol.*, vol. 60, no. 6, pp. 2195 – 2215, Mar. 2015.

[61] J. Song, *et al.*, " Large improvement of the electrical ultrasound (HIFU) phased arrays using multilayer piezoelectric ceramics coupled in lateral mode," *IEEE Trans. on Ultrasound, Ferroelectrics, and Frequency Control*, vol. 59, no. 7, pp. 1584 – 1595, Jul. 2012.

[62] N. P. K. Ellens, *et al.*, "A novel, flat, electronically-steered phased array transducer for tissue ablation: preliminary results," *Phys. Med. Biol.* Vol. 60, no. 6, pp. 2195 – 2215, 2015.

[63] N. R. Draper, and H. Smith, "Fitting a straight line by least squares," in *Applied regression analysis*, 3rd ed. New York, NY, USA, Wiley, 2014, ch. 1, sec. 1.7, pp. 40 – 44.

[64] J. A. Hanley, and B. J. McNeil, "The meaning and use of the area under a receiver operating characteristic (ROC) curve," *Radiology*, vol. 143, pp. 29 – 36, Apr. 1982.

[65] K. Hajian-Tilaki, "Receiver operating characteristic (ROC) curve analysis for medical diagnostic test evaluation," *Caspian J. Intern. Med.*, vol. 4, no. 2, pp. 627 – 635, 2013.